National Library of Canada
Bibliothèque nationale du Canada

Canadian Theses Service
Service des thèses canadiennes

Ottawa, Canada
K1A 0N4

NOTICE

The quality of this microform is heavily dependent upon the quality of the original thesis submitted for microfilming. Every effort has been made to ensure the highest quality of reproduction possible.

If pages are missing, contact the university which granted the degree.

Some pages may have indistinct print especially if the original pages were typed with a poor typewriter ribbon or if the university sent us an inferior photocopy.

Reproduction in full or in part of this microform is governed by the Canadian Copyright Act, R.S.C. 1970, c. C-30, and subsequent amendments.

AVIS

La qualité de cette microforme dépend grandement de la qualité de la thèse soumise au microfilmage. Nous avons tout fait pour assurer une qualité supérieure de reproduction.

S'il manque des pages, veuillez communiquer avec l'université qui a conféré le grade.

La qualité d'impression de certaines pages peut laisser à désirer, surtout si les pages originales ont été dactylographiées à l'aide d'un ruban usé ou si l'université nous a fait parvenir une photocopie de qualité inférieure.

La reproduction, même partielle, de cette microforme est soumise à la Loi canadienne sur le droit d'auteur, SRC 1970, c. C-30, et ses amendements subséquents.

NL-339 (r. 88/04) c

Canada

National Library of Canada
Bibliothèque nationale du Canada

Canadian Theses Service
Service des thèses canadiennes

Ottawa, Canada
K1A 0N4

The author has granted an irrevocable non-exclusive licence allowing the National Library of Canada to reproduce, loan, distribute or sell copies of his/her thesis by any means and in any form or format, making this thesis available to interested persons.

L'auteur a accordé une licence irrévocable et non exclusive permettant à la Bibliothèque nationale du Canada de reproduire, prêter, distribuer ou vendre des copies de sa thèse de quelque manière et sous quelque forme que ce soit pour mettre des exemplaires de cette thèse à la disposition des personnes intéressées.

The author retains ownership of the copyright in his/her thesis. Neither the thesis nor substantial extracts from it may be printed or otherwise reproduced without his/her permission.

L'auteur conserve la propriété du droit d'auteur qui protège sa thèse. Ni la thèse ni des extraits substantiels de celle-ci ne doivent être imprimés ou autrement reproduits sans son autorisation.

ISBN 0-315-55502-5

Canada

THE UNIVERSITY OF ALBERTA

PHASE RELATIONS OF AL-UNDEPLETED AND AL-DEPLETED KOMATIITES

BY

Kejian Wei

A THESIS

SUBMITTED TO THE FACULTY OF GRADUATE STUDIES AND RESEARCH IN PARTIAL FULFILIMENT OF THE REQUIREMENTS FOR THE DEGREE OF MASTER OF SCIENCE

DEPARTMENT OF GEOLOGY

EDMONTON, ALBERTA

FALL, 1989

THE UNIVERSITY OF ALBERTA

RELEASE FORM

TITLE OF THE AUTHOR: Kejian Wei

TITLE OF THESIS: PHASE RELATIONS OF AL-UNDEPLETED AND AL-DEPLETED KOMATIITES AT 4 TO 12 GPa

DEGREE: MASTER OF SCIENCE

YEAR OF THIS DEGREE GRANTED: FALL, 1989

Permission is hereby granted to **THE UNIVERSITY OF ALBERTA LIBRARY** to reproduce single copies of this thesis and to lend or sell such copies for private, scholarly or scientific research purposes only.

The author reserves other publication rights, and neither the thesis nor extensive extracts from it may be printed or otherwise reproduced without the author's written permission.

Kejian Wei.....

PERMANENT ADDRESS:

DEPARTMENT OF GEOLOGY

THE UNIVERSITY OF ALBERTA

EDMONTON, ALBERTA

CANADA, T6G 2E3

DATE: August 11, 1989

THE UNIVERSITY OF ALBERTA

FACULTY OF GRADUATE STUDIES AND RESEARCH

The undersigned certify that they have read, and recommend to the Faculty of Graduate Studies and Research for acceptance, a thesis titled **Phase Relations of Al-undepleted and Al-depleted Komatiites at 4 to 12 GPa** submitted by Kejian Wei in partial fulfilment of the requirements for the degree of MASTER OF SCIENCE.

Committee Chairman and Co-Supervisor:

Dr. K. Muehlenbachs .....

Supervisor:

Dr. R. G. Tronnes .....

Committee Members:

Dr. B. E. Nesbitt .....

Dr. D. R. Schmitt .....

Dr. C. T. Herzberg .....

Dr. D. C. Presnall .....

Date: August 11, 1989

DEDICATION

This thesis is dedicated to the memory of Chris Scarfe

ABSTRACT

The anhydrous phase relations of natural Al-undepleted komatiite (AUK) with 25 % MgO and Al-depleted komatiite (ADK) with 32 % MgO have been investigated over the pressure range from 4 to 12 GPa, using samples from Munro Township, Ontario and Barberton Mountain Land of South Africa, respectively. All experiments were carried out with graphite or molybdenum capsules in a uniaxial split-sphere apparatus and 18 mm octahedral pressure cell. The thermal gradient within the central part of the sectioned furnace is estimated to be about 50 °C/mm near the junction of the thermocouple.

For both of the compositions the liquidus phase is olivine at low pressure, clinopyroxene in an intermediate pressure range and garnet at high pressure. Olivine-clinopyroxene liquidus cosaturation occurs at 5.2 GPa for the AUK and 9.6 GPa for the ADK, and the clinopyroxene-garnet cosaturation point is at 6.8 GPa for AUK and at 11.5 GPa for ADK. The subsolidus assemblage comprises olivine, clinopyroxene and garnet in the entire pressure range (4-12 GPa) for both of the compositions, and the last phase to crystallize with decreasing temperature is garnet at pressures below the clinopyroxene liquidus interval and olivine at higher pressures.

Assuming that both of the komatiites represent near primary melt compositions and that the melt separated from residues involving olivine, the maximum pressures of magma separation would be 5.2 GPa and 9.6 GPa for AUK and ADK, respectively. The absence of garnet from the olivine-clinopyroxene liquidus cosaturation points implies that garnet was not a residual phase and that the melting was not pseudoinvariant. 10-30 % of melting of mantle peridotite at pressures corresponding to the olivine-clinopyroxene cosaturation points, i. e. at depth of 160 km and 300 km, can generate the AUK and ADK, respectively. Small amounts of garnet originally present in the source peridotites were likely consumed during the melting. The chemical characteristics of the ADK (high Ca/Al

and Gd/Yb) were probably acquired by gravitational segregation of garnet from a rising peridotite diapir prior to melt separation.

ACKNOWLEDGEMENTS

This thesis is dedicated to the memory of Chris Scarfe, who was my initial supervisor and discussed the project with me.

I am very grateful to Reidar Tronnes for his supervision and guidance with valuable advice and expertise throughout the course of this study, and for his careful review of this manuscript.

Many special thanks go to Karlis Muehlenbachs, my cosupervisor, for his kind help and constant encouragement throughout difficult situations.

I acknowledge Eiich Takahashi and Dante Canil for introducting me to the multianvil press and piston cylinder apparatus and for valuable suggestions, to Claude Herzberg for his encouragement and thoughtful suggestions and to N. T. Arndt, Max-Planck-Institut fur Chemie, Mainz and H. S. Smith, University of Cape Town, for kindly providing the samples used as starting materials. Helpful discussions and suggestions by Masami Kanzaki and Dean Presnall and technical assistance by Diane Caird, John Machacek, Paul Wagner, David Tomlinson and Frank Dimitrove are greatly appreciated. Claude Herzberg also made his preprint available to me.

The study was financially supported by graduate fellowships from Academia Sinica and University of Alberta and equipment and operating grants from by Natural Sciences and Engineering Research Council of Canada (SMI-105, CH0006947 and OGP0008394 to C. M. Scarfe and OGP0041766 to R. G. Tronnes) and University of Alberta.

TABLE OF CONTENTS

Chapter	Page
Dedication	**IV**
Abstract	**V**
Acknowledgements	**VII**
List of Tables	**X**
List of Figures	**XI**
I. Introduction	**1**
II. Starting Materials	**5**
III. Experimental Methods	**7**
1. High pressure apparatus and furnace assembly	7
2. Sample containers	7
3. Pressure calibration and temperature monitoring	8
4. Experimental and analytical procedures	8
5. Temperature distribution within the furnaces	9
IV. Experimental Results	**12**
1. Phase relations	12
2. Liquidus phase composition	13
V. Discussion	**16**
1. Absence of orthopyroxene	16
2. Possible residual minerals	17
3. High MgO content and high CaO/Al_2O_3 values	18
VI. Conclusion	**21**

VII. References 38

LIST OF TABLES

Page

Table 1 General Features of Al-undepleted and Al-depleted Komatiites and Compositions of Starting Materials 22

Table 2 Experimental Conditions and Results 23

Table 3 Microprobe Analyses of Olivines in Experimental Runs 24

Table 4 Microprobe Analyses of Clinopyroxenes and Garnets in Experimental Runs 25

LIST OF FIGURES

Page

Figure 1 Weight percent oxide variation diagrams for representative samples of Al-undepleted komatiites (AUK) and Al-depleted komatiites (ADK) 26

Figure 2 Cross section of the furnace assemblies 27

Figure 3 Back scattered electron SEM photomicrographs of run products 28

Figure 4 Temperature distribution within two-pyroxene charges from an experiment at 1500 °C (thermocouple reading) and 7 GPa using a sectioned graphite heater (Figure 2B) 32

Figure 5 Phase diagrams of the Al-undepleted (AUK) and Al-depleted (ADK) komatiites (samples M620 and HSS-15, respectively) 33

Figure 6 Distribution coefficient ($K_{d(Fe/Mg)^{(ol/bulk\ komatiite)}}$) of Fe/Mg between liquidus olivine and bulk komatiitic liquid as function of pressure 34

Figure 7 Al_2O_3 content of clinopyroxene as a function of pressure 35

Figure 8 Komatiite compositions projected from enstatite (MS) onto the plane M_2S-C_2S_3-A_2S_3 in the system CMAS (CaO-MgO-Al_2O_3-SiO_2) 36

Figure 9 Schematic diapir model for the origin of Al-undepleted and Al-depleted komatiites 37

I. Introduction

The existence of ultramafic liquid had been questioned for a century before Viljoen and Viljoen (1969a) discovered the first komatiite in 1969. Named after the discovery site near the Komati river in the Barberton Mountain Land of South Africa, komatiites have since been found in other parts of the world, e.g. in Australia (McCall and Leishman, 1971; Williams, 1972) and Canada (Pyke et al, 1973). These rocks commonly occur as major components in Archean greenstone belts with ages ranging from 2.5 to 3.6 Ga (see Arndt, 1979), indicating that komatiitic magmatism might have played an important role in the chemical differentiation of the Archean mantle. Information about their petrogenesis is therefore essential for our understanding of the geochemical and geophysical characteristics of the Archean mantle.

Various models have been proposed to explain the unusually high magnesium contents (18-34 % MgO) of the komatiitic liquids. Viljoen and Viljoen (1969a, b), Green (1975), Cawthorn and Strong (1974), Sun and Nesbitt (1978), Nesbitt et al. (1979) and Jahn et al. (1980), for instance, suggested that the high magnesium liquids were generated by high degree (up to 70 %) of partial melting of a mantle source at relatively shallow level. Arguing that the high degree melting model is not supported by the low viscosities of such liquids, Arndt (1977) and Arth et al. (1977) proposed a sequential melting model in which an ultrabasic magma was formed by further partial melting of a refractory residue containing small amounts of trapped basic liquid after an initial basic magma separation. Bickle et al.(1977) suggested that komatiites are liquids that separated from a dunitic or harzburgitic source, and later assimilated a portion of the crystalline residue during ascent. There are also several studies suggesting low degrees of pseudoinvariant melting at very high pressures. During their melting experiments, Takahashi and Scarfe (1985), Scarfe and Takahashi (1986) and Takahashi (1986)

observed that liquids formed by partial melting of peridotite at its solidus become more magnesian with increasing pressure and that a komatiitic liquid was produced at 5-7 GPa leaving olivine (ol), clinopyroxene (cpx) and garnet (ga) in the residual source. Herzberg and O'Hara (1985) and Herzberg and Ohtani (1988) examined the locations of komatiites in liquidus projection diagrams in the pseudoquaternary system CaO-MgO-Al_2O_3-SiO_2 and noticed that the komatiites are distributed near the experimentally determined pseudoinvariant melting points of peridotite. They suggested, accordingly, that komatiites could have been formed by pseudoinvariant melting (ol+cpx+ga+liquid).

Nesbitt et al. (1979) divided komatiites into aluminum undepleted komatiites (AUK) and aluminum depleted komatiites (ADK). The chemical characteristics of the different types are shown in Table 1 and Figure 1. The AUKs commonly have a CaO/Al_2O_3 ratio of about one (close to mantle peridotitic value), an Al_2O_3/TiO_2 ratio of about 20 (close to chondritic value) and flat heavy rare earth element pattern ($(Gd/Yb)_n$ about 1). Most komatiites such as those from Munro Township, Ontario and Belingwe, Zimbabwe, belong to this type. In contrast, ADKs usually have high CaO/Al_2O_3 (about 1.6), low Al_2O_3/TiO_2 (about 11) and depleted heavy rare earth element pattern ($(Gd/Yb)_n$ about 1.4). A few old (about 3.5 Ga) high magnesium rocks including the classic Barberton komatiites belong to this type.

Because garnet and clinopyroxene are the major host minerals for aluminum and the rare earth elements in the upper mantle, the compositional difference between AUK and ADK has been explained by varying degrees of garnet and clinopyroxene involvement during melting or later fractionation. Cawthorn and Strong (1974) suggested that the contrasting compositions are due to the clinopyroxene/garnet ratio in the original peridotitic source. Arndt (1977), Arndt et al.(1977) and Arth et al. (1977), however, argued that the chemical signature of komatiites is mainly a function of the relative proportion of garnet and clinopyroxene retained in their residue. On the other

hand, Green (1975), Sun and Nesbitt (1978) and Nesbitt et al. (1979) suggested that the removal of garnet from the source could explain the depletion of aluminum. More recently, Ohtani (1984) and Herzberg and Ohtani (1988) proposed that Al-undepleted komatiites and Al-depleted komatiites were formed at different depths.

Most of the previous studies of the origin of komatiites have concentrated on the geochemistry (e.g. major elements, trace elements and isotopic ratios) of komatiites. These investigations have placed some constraints on the chemical characteristics of the sources of komatiites, but the depth of komatiite derivation and the residual mineral assemblage of their source are still uncertain. The additional information about the phase relationships of komatiite as a function of pressure is therefore required in order to place some constraints on these genetic problems.

Green et al.(1975) first determined the liquidus of a komatiitic sample (49 J) from Barberton Mountain Land of South Africa at pressures from 0.2 to 2.5 GPa under hydrous condition and from 0.2 to 1.0 GPa under anhydrous condition. Their experimental results show that the liquidus phase is olivine with normative forsterite of about 93 and the one-atmosphere liquidus temperature is about 1650 °C for this komatiite with 32.97 % MgO. Arndt (1976) studied the phase relationships of Al-undepleted komatiites with 25 % MgO from Munro township, Ontario, within the melting interval at pressures below 4 GPa under anhydrous condition. The olivine is the only liquidus phase at all studied pressures. The second phase that crystallized with olivine was calcium-poor pyroxene (2-3 GPa) or spinel (< 2GPa). Garnet appears near the solidus at about 3 GPa, but appears to become the second crystallizing phase replacing pyroxene at high pressure. Bickle et al (1977) carried out some experiments on Al-undepleted komatiites from Belingwe greenstone belt and found that all samples have olivine as liquidus phase at pressures below 4 GPa, except one sample having orthopyroxene as liquidus phase between 1 and 4GPa.

If komatiites were formed by pseudoinvariant melting as suggested by Herzberg and O'Hara (1985), Takahashi and Scarfe (1985), Scarfe and Takahashi (1986), Takahashi (1986) and Herzberg and Ohtani (1988), the pressure of komatiite derivation would be higher than 4 GPa and the multiple saturation points could be found at somewhere above that pressure. Examination of the phase relationships of a "primary " komatiite at pressures above 4 GPa, therefore, can provide further constraints on:

a. The residual mineral assemblages from which the komatiitic magma was extracted;

b. The pressure and temperature under which the magma could have been separated;

c. The partitioning of elements between residual phases and the magma.

This thesis presents experimental data on the anhydrous phase relations of both Al-undepleted and Al-depleted komatiites at pressures from 4 to 12 GPa. Based on the experimental results, the major problems concerning petrogenesis of komatiites such as high MgO content and high CaO/Al_2O_3 value are discussed.

II. Starting Material

Two natural samples, M620 and HSS-15, were used as starting materials for Al-undepleted komatiite and Al-depleted komatiite, respectively. The compositions of the two chosen samples are listed in Table 1.

The sample M620 was collected from a spinifex-textured komatiitic lava in Munro Township, Ontario (Arndt and Nesbitt, 1984). This sample contains 25 wt% MgO and has Al/Ti and Ca/Al ratios close to the average of Al-undepleted komatiite (Table 1). M620 displays typical spinifex texture with skeletal blades of olivine pseudomorphs (10-15 mm long but only 0.3-1 mm wide) randomly oriented in a matrix of fine skeletal clinopyroxene and devitrified glass. The olivine has been entirely replaced by fine grained hydrous minerals, but most clinopyroxene remains fresh. Detailed descriptions of field geology, petrology and geochemistry of the komatiites from this area have been given by Pyke et al.(1973), Arndt et al. (1977), Arth et al. (1977), Arndt and Nesbitt (1982) and Arndt and Nesbitt (1984). A Sm-Nd age of 2.6 Ga for komatiites from Munro Township was provided by Zindler (1982). Although M620 has not been investigated experimentally, a sample (SA 3091) of composition similar to M620 from the same area was used in the experiments by Arndt (1976).

The sample HSS-15 was collected from a chilled margin of a pillow lava or flow top breccia in the Barberton Mountain Land of South Africa (Smith and Erlank, 1982; Smith, 1988, personal communication). The chemical analyses (Table 1) show that this sample contains 31.5 wt % MgO and has Ca/Al and Al/Ti ratios close to the average of Al-depleted komatiites. HSS-15 is aphanitic with less than 0.4 mm microphenocrysts of olivine, pseudomorphed by serpentine. The geology of Barberton Mountain Land was described by Anhaeusser (1973, 1978), Anhaeusser et al. (1968), Viljoen and Viljoen

(1969 a, b, c), Viljoen et al.(1982) and Williams and Furnell (1979) and detailed petrological and geochemical accounts of the komatiites were provided by Nesbitt et al. (1979), Jahn et al.(1982) and Smith and Erlank (1982). Sm-Nd ages of about 3.6 Ga were provided by Hamilton et al. (1979) and Jahn et al. (1982). A sample (J49) from same area was used in the experiment by Green et al.(1975).

Based on their textures, structures and compositions, it was assumed that these two natural samples represent liquids close to primary magmas in composition.

III. Experimental Methods

1. High pressure apparatus and furnace assembly

All experiments were performed at the University of Alberta with a 2000 ton uniaxial split sphere apparatus (see Ito et al., 1984 for description). A semisintered MgO-Cr_2O_3 (5%) octahedron was used as pressure medium between 8 cubic tungsten carbide anvils (32.5mm side lengths) with truncated corners (11 mm truncation edge).

The furnace assemblies used in this study are shown in Figure 2. The ZrO_2 sleeve acts as a heat insulator and together with the pressure medium improves the efficiency of the graphite or $LaCrO_3$ heaters. Graphite heaters were used in most of the experiments below 7 GPa. However, at the highest pressures and temperatures used in this study the increased kinetics of the graphite to diamond transition prevents the use of graphite heaters. $LaCrO_3$ with its temperature dependent resistance (Takahashi, 1986) and thermal insulating capacity provides a heater with slightly lower power consumption and lower thermal gradient than a graphite heater.

2. Sample containers

The sample container was made of graphite for all runs below 9 GPa and of molybdenum for most runs above that pressure in order to prevent diamond formation. No special measure was taken to buffer the oxygen fugacity, but by analogy with the lower pressure studies by Biggar (1970), Thompson and Kushiro (1972) and Visser and Koster Van Groos (1979), the graphite and molybdenum capsules may impose oxygen fugacities between the magnetite-wustite and iron-wustite buffers and near the iron-wustite buffer, respectively. No metallic iron or molybdenum alloy was observed, and no iron loss to the molybdenum capsules was detected by electron microprobe analyses in the run products of this study.

3. Pressure calibration and temperature monitoring

The sample pressure was calibrated against the load tonnage by using the following transitions:

a. At room temperature: Bi (I-II) at 2.55 GPa (Hall, 1971) and Bi(V-VI) at 7.7 GPa (Homan, 1975);

b. At 1000 °C: Fe_2SiO_4 (α-γ) at 5.3 GPa (Yagi et al., 1987) and coesite-stishovite at 9.4 GPa (Suito, 1977);

c. At 1500 °C and 2000 °C: quartz-coesite at 3.6 and 4.2 GPa, respectively (Boyd and England, 1960; Mirwald and Massonne, 1980).

Because the shift of the calibration curve between 1000 °C and higher temperature (1500 °C or 2000 °C) does not exceed the uncertainty of the calibration, all run pressures were measured based on the pressure calibration at 1000 °C. The accuracy and precision of the sample pressure is estimated to be $\pm$ 0.2 GPa.

The temperature was monitored with a W3%Re/W25%Re thermocouple which passed through the center of the furnace and was electrically insulated from the heater by alumina sleeves (see Figure 2). No correction for the effect of pressure on the thermocouple emf was made. According to Getting and Kennedy (1970), Herzberg et al.(1989) and the two-pyroxene thermometer experiments of this study (see below), the recorded temperatures may be 50-100 °C lower than the real temperature in the hot end of the sample capsules. Using a programmable controller, the temperature could be controlled to within $\pm$ 5 °C.

4. Experimental and analytical procedures

Each sample was ground in an agate mortar under alcohol until the grain size was less than 5-10 μm. The pulverized samples were fired at 1100 °C in Ar atmosphere for three hours and stored in an oven at 110 °C.

Approximately 10-20 mg fired powder was loaded in a capsule which was then covered with a lid. Two capsules were placed in the internal graphite resistance furnace and insulated from the furnace with MgO sleeves and spacers. The whole assembly (Figure 2) installed in the MgO-Cr_2O_3 octahedron was fired at 1000-1100 °C in Ar atmosphere for one hour in order to completely dehydrate all of the parts. The assembly was subsequently installed between the tungsten carbide anvils, and the inner anvil configuration was loaded in the space between the outer split-sphere anvils.

The sample pressure was increased by 0.1 to 0.2 GPa per minute to the run pressure, and the temperature was then raised by 100 °C per minute to the desired value. The experiments were quenched by cutting power and the quench time (from run temperature to 400 °C) was 2-3 seconds.

The phases in the run charges exposed on polished surfaces were identified by optical microscope and back scattered electron imaging at the University of Alberta. Selected liquidus phases were analyzed by electron microprobe at the University of Calgary, using 15 kV acceleration voltage and 10-15 nA beam current. The counting time was 20 seconds on peaks and background. The major elements (Si, Ti, Al, Mn, Fe, Mg, Ca and Na) were measured simultaneously by using eight wave length dispersive spectrometers. Data reduction and correction were made with the Bence and Albee (1968) computer program with modification of Albee and Ray (1970). The analytical accuracy and precision (one standard deviation) is ±1.5 % of the amount present for oxides comprising more than 5 %, ±2-30 % for oxides in the 1-5 % range and ±3-50 % for oxides comprising less than 1 % of the analysis.

5. Temperature distribution within the furnaces

Figure 2 shows the two different types of heaters used in this study: a simple cylindrical heater of $LaCrO_3$ (A) and a sectioned heater of graphite (B). Some of the experiments were also performed with simple cylindrical graphite heaters or with sectioned $LaCrO_3$ heaters. A disadvantage of using simple cylindrical heaters is the large axial temperature gradient within a charge. According to measurement by Takahashi et al. (1982) using the two pyroxene thermometer method, the temperature gradient in the simple cylindral furnace is as high as 200 °C/mm. The large temperature gradient was also observed in the early experiments of this study using the simple cylindrical furnaces. One example is given by the run product from experiment 135 (HSS-15) at 5 GPa and 1770 °C (Figure 3a). In this charge, the area within 0.1 mm of the thermocouple (hot spot) is 100 % quenched liquid (glass+ quenched olivine). Towards the cooler end of the capsule are zones of ol+liquid, ol+cpx+liquid, ol+cpx+ga+liquid and ol+cpx+ga. A large thermal gradient may therefore provide useful information on the near liquidus and near solidus phase relations in one single experimental charge, but it clearly causes a large temperature uncertainty.

The sectioned heater (Figure 2B, see also Fujii et al., 1989) was designed in order to reduce the thermal gradient, and was used in most experiments. The furnace B is similar to furnace A, except that the simple cylindrical sleeve of graphite or $LaCrO_3$ is replaced by three short sleeves. The middle sleeve is made so that its thickness is twice as large as that of the other two end sleeves. The thermal effect of this type of heater is similar to that produced by a tapered heater (Kushiro, 1976; Takahashi et al., 1982).

Two experiments were carried out with sectioned graphite heaters to map the temperature distribution within the sample capsules, using the two-pyroxene thermometer method described by Takahashi et al. (1982). A mixture of crystalline enstatite and diopside was equilibrated at 5 and 7 GPa and 1500 °C (thermocouple reading) for 140 and 210 minutes, respectively, and the compositions of the coexisting pyroxenes were measured at different locations throughout the samples. Figure 3b

shows the run products comprising an equilibrium texture intergrowth between orthopyroxene and clinopyroxene at 7 GPa and 1500 °C. The spatial distribution of K_d ($=(1-X^1_{Ca})^{opx}/(1-X_{Ca})^{cpx}$) values and corresponding temperatures according to the Nickel et al. (1985) thermometer are shown in Figure 4. The variation of the K_d within 1 mm of the hot end of the capsule ranges from 0.28 to 0.46, and the temperature variation within the same area is about 50 °C. The temperature uncertainty inherent in thermometer is ± 25 °C (Nickel et al., 1985). Independent experiments with a similar furnace design and two axial thermocouple pairs show that the axial thermal gradient is less than 10 °C/mm near the center of the furnace (M. Kanzaki, personal communication).

The thermometer values at the hot ends of the capsules in both runs are 50-100 °C higher than the thermocouple reading (Figure 4). This may be due to the local temperature perturbations related to the resistance pattern of the heater in the area of thermocouple penetration (Herzberg et al., 1989). It is also possible that the thermocouple with sleeves represents an avenue for elevated heat radiation from the furnace.

---

[1] Mole fraction of calcium

IV. Experimental results

The phase assemblages listed in Table 2 represent the coexisting phases observed within 0.4 mm and 0.10 mm of the hot end of the capsules for sectioned heaters and simple cylindrical heaters, respectively. In these portions of the samples the temperature drop from the hot end is less than 25 °C. The run durations, mostly of 5 to 30 minutes (Table 2), were sufficient to produce large (>20μm), unzoned and composionally homogeneous crystals within the liquidus-solidus interval. Figure 3 (a, c, d, e) shows backscattered electron images of some of the run products. Almost all of the run products from suprasolidus experiments show an increasing proportion of melt towards the center of the furnace. Quenched crystals always formed in the liquid portions of the samples. The distribution of melt (quenched crystals) and equilibrium crystals are independent of whether the sample capsule was above or below the central hot spot, indicating that gravitational separation is not important.

1. Phase relations

The phase relations of the two types of komatiite are shown in Figure 5. There are only three solid phases present in the investigated pressure range: olivine (ol), clinopyroxene (cpx) and garnet (ga). Orthopyroxene is absent even in the subsolidus region.

Al-undepleted komatiite (Figure 5, AUK): The liquidus phase is olivine at pressure below 5.2 GPa, clinopyroxene between 5.2 and 6.8 GPa and garnet above 6.8 GPa. The komatiitic liquid is cosaturated with olivine and clinopyroxene at 5.2 GPa, and with clinopyroxene and garnet at 6.8 GPa. The crystallization sequence with decreasing temperature is ol+liq (liquid)→ ol+cpx+liq→ ol+cpx+ga+liq→ ol+cpx+ga at pressures

below the ol+cpx cosaturation point and ga+liq→ ga+cpx+liq→ ga+cpx+ol+liq→ ga+cpx+ol at pressures above the cpx+ga cosaturation point. The second crystallizing phase in the pressure range between the two cosaturation points is olivine and garnet below and above 6.1 GPa, respectively. The liquidus-solidus interval decreases from 135 °C at 4 GPa to 75 °C at 12 GPa.

Al-depleted komatiite (Figure 5, ADK): The changes of liquidus phase with increasing pressure and the crystallization sequence of phases with decreasing temperature are similar to those for the Al-undepleted komatiite. The most striking feature of the phase relationship of Al-depleted komatiite is the high pressures of its ol+cpx and cpx+ga cosaturation points (at 9.6 and 11.5 GPa, respectively). Moreover, its liquidus temperature is slightly higher than that of the Al-undepleted komatiite at a given pressure. Minima of about 50 °C for the liquidus and solidus interval are reached at the olivine-clinopyroxene and clinopyroxene-garnet cosaturation points in this type rock.

2. Liquidus phase compositions

In order to evaluate the mineral-melt interaction related to partial melting or fractional crystallization of komatiites, I tried to obtain representative analyses of the minerals that crystallized in equilibrium with a liquid of composition identical or very similar to the bulk komatiite. Reconnaissance analyses of the 100 % quenched liquid portions (hot zones) of some of the experimental charges in different run durations were performed in order to investigate whether the bulk composition is maintained within each segment of the charges. The small scale inhomogeneous quench texture required raster type analyses covering areas of about 100 μm^2. These analyses seem to indicate that there was no significant mass transportation of the type suggested by Walker et al.(1988) and Lesher and Walker (1988) along the axial thermal gradient in the furnaces within the run durations used in this study. Based on this observation I analyzed the liquidus

phases that are located at the border to the 100 % liquid portions of the charges, and in particular the crystals that are isolated from other crystals by intervening quenched liquid (e. g. Figure 3c).

Olivine (see Figure 3c, d): The olivine compositions are given in Table 3. The forsterite (Fo) contents of liquidus olivines range from 88 to 93. The Fe-Mg distribution coefficient (K_d[2] (Fe/Mg)) values of the olivines in equilibrium with a liquid of bulk komatiite composition increases slightly as a function of increasing pressure, except for the analyses (HSS-15, 135, 138) with K_d value of about 0.6. The other K_d values as well as the observed increase with increasing pressure are in accordance with the results by Ulmer (1989) and Takahashi and Kushiro (1983) (Figure 6).

Clinopyroxene (see Figure 3d, e): The clinopyroxene compositions are listed in Table 4. They are subcalcic (mol % wollastonite of 5-19) with highly variable aluminum contents. The partitioning coefficient ($D^3_{Al(cpx/bulk\ komatiite)}$)of aluminum between clinopyroxene and komatiitic liquid decreases slightly with increasing pressure in the 4 to 11 GPa range. This is in accordance with the results of Takahashi (1986) and Scarfe and Takahashi (1986) who found a pronounced decrease in the aluminum content of clinopyroxene with increasing pressure (Figure 7). The $D^4_{Ca(cpx/bulk\ komatiite)}$ ranges from o.45 to 1.73 and is higher at high pressure than at low pressure.

Garnet: Unlike the large and euhedral liquidus olivine (20-80 μm) and clinopyroxene (10-40 μm) crystals, the garnets are generally small (less than 15 μm) and rounded. The

---

2 $K_d=(FeO/MgO)^{ol}/(FeO/MgO)^{bulk\ komatiite}$

3 $D_{Al}=(Al2O3)^{cpx}/(Al2O3)^{bulk\ komatiite}$

4 $D_{Ca}=(CaO)^{cpx}/(CaO)^{bulk\ komatiite}$

liquidus garnet are pyrope dominated, and they contain a significant pyroxene component (Table 4).

V. Discussion

The most important findings of this investigation are the following:

a. Al--undepleted and Al-depleted komatiites are cosaturated with olivine and clinopyroxene at 5.2 GPa and 9.6 GPa, and with clinopyroxene and garnet at 6.8 GPa and 11.5 GPa, respectively. No garnet is present at liquidus coexisting with olivine.

b. The subsolidus assemblage comprises olivine, clinopyroxene and garnet. No orthopyroxene was present in the pressure range investigated.

c. The partitioning of Fe and Mg between olivine and komatiitic liquid and the partitioning of Al and Ca between clinopyroxene and komatiitic liquid are dependent on pressure.

If the principal assumption, namely that the composition of starting materials (M620, HSS-15) are representative of nearly primary magma, is correct, these phase relationships can be used to place some constraints on the origin of Al-undepleted and Al-depleted komatiites.

1. Absence of orthopyroxene

The Earth's mantle is dominantly peridotitic at least above the 400 km discontinuity (Ringwood, 1975; Anderson, 1988), and the volumetrically most important phases down to about 100 km depth are olivine and low calcium orthopyroxene. However, in the 100-400 km depth range the abundances of clinopyroxene and garnet increase at the expense of orthopyroxene, whereas olivine remains the dominant phase (Ito and Takahashi, 1987). Due to the increased solubility of the enstatite component in clinopyroxene and garnet with increasing temperature and pressure, respectively (Nickel and Brey, 1984; Yamada and Takahashi, 1984; Kanzaki, 1987), the mineral assemblages of most peridotites are reduced to olivine, garnet and high calcium

clinopyroxene at solidus conditions above 3-5 GPa (Takahashi, 1986; Scarfe and Takahashi, 1986). This is confirmed by the absence of orthopyroxene in our high pressure and high temperature experiments (Figure 5) and the significant enstatite component of the liquidus garnets (Table 4).

2. Possible residual minerals

The minerals present in the residue of a primary melt will crystallize at the liquidus of that composition at conditions of melt generation, unless one of the minerals was in reaction relation with the liquid (Wyllie et al., 1981; Wyllie, 1984). The pseudoinvariant melting of peridotite change from peritectic to eutectic-like at pressures of about 3 GPa (Irvine and Sharpe, 1982; Herzberg, 1983; Herzberg et al., 1989). The lack of pseudoinvariant cosatuation points for the two investigated compositions (Figure 5) indicate that they may have been generated along the olivine-clinopyroxene cotectic or the clinopyroxene-garnet cotectic.

Melting experiments using peridotitic and chondritic compositions have shown that although the behavior of most mantle minerals varies with pressure and temperature, olivine is always the last phase which is completely exhausted during melting at pressure up to 14-16 GPa (Takahashi, 1986; Ito and Takahashi, 1987; Ohtani et al, 1986). Therefore, clinopyroxene only, garnet only, or clinopyroxene and garnet should be rejected as residual assemblages. A large degree of partial melting leaving olivine as the only residual phase is possible, and has been suggested as a mechanism of komatiite magma generation (e.g. Viljoen and Viljoen, 1969a, b; Green, 1975; Jahn et al., 1980; Nisbet and Walker, 1982). However, the large thermal perturbations required for the process, combined with the low melt viscosities (see Arndt, 1977, Nisbet, 1982) indicate that this is an unlikely scenario.

The compositional variation of various Al-undepleted and Al- depleted komatiites points to olivine and /or clinopyroxene control during melting or later fractionation

(Cawthorn and Strong, 1974; Bickle et al., 1977, Nesbitt et al., 1979, Smith and Erlank, 1982). In Figure 1, the compositions of experimental liquidus phases are plotted along with the compositions of representative komatiite samples in Al_2O_3 and CaO versus MgO variation diagrams. The liquidus olivine and clinopyroxene compositions plot close to the least squares linear regression lines for these komatiite compositions, whereas the garnet compositions deviate significantly from the lines, indicating that garnet crystallization was not important in the generation of the compositional spectra.

Least squares mass balance modelling using the pyrolite and KLB-1 compositions (Table 1) as source rocks, the AUK (M620) and ADK (HSS-15) as derivative liquids and various olivines and clinopyroxenes (Table 3 and 4) as residual phases, suggests that 10-30 % partial melting of a mantle source leaving residues comprising about 65 % olivine and 35 % clinopyroxene could yield the komatiitic liquids. Considering the subsolidus assemblage (Figure 5) and such melt fractions, it is possible that small amounts of garnet which were likely present in the AUK source, were consumed by melting. This will explain the Al- and HREE undepleted nature of this komatiite (Table 1).

3. High MgO content and CaO/Al_2O_3 values

If, as suggested above, the two types of komatiite were formed by melting at olivine-clinopyroxene liquidus cosaturation points at 5.2 GPa (about 160 km) and 9.6 GPa (about 300km), respectively, it would be tempting to explain their compositional difference by contrasting residual mineral chemistry at different pressures. The critical compositional difference between AUK and ADK, the higher MgO content and the higher Ca/Al ratio in the ADK (see Table 1), must be addressed.

O'Hara et al. (1975), Herzberg and O'Hara (1985) and Herzberg and Ohtani (1988) have approached the problem of high magnesium contents of komatiites using

the CMAS (CaO-MgO-Al_2O_3-SiO_2) polybaric liquidus phase diagrams. They found that the komatiites were distributed along a line formed by pseudoinvariant points toward the olivine corner (Figure 8), suggesting that the compositional spectrum of komatiites is caused by pseudoinvariant melting of mantle peridotites at different pressures. The starting materials used in this study are also projected in Figure 8. The compositions of M620 and HSS-15 plot near pseudoinvariant points (ol+py+ga+l) at about 5-6 GPa and 9-10 GPa, respectively. The agreement between the positions of the starting materials in the CMAS diagram and the pressure conditions of their olivine+clinopyroxene cosaturation points (See Figure 5) confirms that the more magnesian liquids could have been formed at higher pressures by partial melting of the same peridotitic source as the less magnesian ones. The increasing $K_{d(Fe/Mg)}$ between olivine and liquid with increasing pressure (Figure 6) also supports this view.

It should be noted, however, that no pseudoinvariant point with simultaneous liquidus saturation of all of the subsolidus phases (ol+cpx+ga) is found along the liquidi of either the Al-undepleted or Al-depleted komatiite. The absence of garnet from the olivine+clinopyroxene cosaturation points suggests that the komatiites were not formed at, but near, the pseudoinvariant points of peridotites.

Olivine contains insignificant amounts of aluminum and calcium (Table 3), and clinopyroxenes in equilibrium with melts at peridotite solidi and komatiite liquidi show nearly constant Ca-content and decreasing Al-content with increasing pressure (Scarfe and Takahashi, 1986, Takahashi, and the results in Table 4 and Figure 7). The increasing Ca/Al ratio from the AUK to ADK can therefore not be explained by the residual olivine-clinopyroxene control at different pressures during melting of the same source composition. Garnet control seems to be required to explain the compositional difference since the $D_{Al(ga/bulk\ komatiite)}$ is much higher than $D_{Ca(ga/bulk\ komatiite)}$ (see

Table 4), but this phase is clearly absent at the olivine-clinopyroxene cosaturation points (Figure 5, ADK).

In order to reconcile the chemical characteristics of the ADK with its observed liquidus relations, this author favour a pre-melting garnet fractionation model shown in Figure 9 which is similar to those of Green (1975), Ohtani (1984), and Takahashi and Scarfe (1985). In this model, garnets are gradually segregated from the upper portions of rising, partially molten peridotite diapirs. Garnet is significantly denser than olivine and pyroxene (about 3.7 g/cm^3 versus 3.3-3.4 g/cm^3 at 10 GPa according to Ohtani, 1984, 1988), and is probably also denser than ultrabasic silicate liquids in the 10-15 GPa pressure range. Olivine, and possibly clinopyroxene may have densities similar to or slightly lower than that of the interstitial melt at these pressures (Herzberg, 1987a, b; Agee and Walker, 1988). Such density relations will favour relative sinking of garnet crystals in a rising diapir containing a small melt fraction. When the melt fraction in the top of the diapir is sufficient for melt extraction, the liquid composition will be buffered by an olivine-clinopyroxene residue and have a garnet depleted signature (i.e. low Al, HREE).

The phase relations of the ADK indicate that the melt may have separated from its diapir at a pressure of 9.6 GPa (300 km depth). This could represent the pressure of density crossover between a komatiitic melt and an olivine dominated residue (see discussions by Nisbet and Walker, 1982; Herzberg, 1987a, b; Agee and Walker, 1988). The model presented in Figure 9 implies, however, that the diapir sources of Al-undepleted komatiites would have started to melt above the density crossover since the geochemical characteristics of AUK requires no fractionation of garnet from the its source.

VI. Conclusions

The main difference between the phase relations of the AUK and ADK is the pressure of the liquidus cosaturation points. Olivine is liquidus phase up to 5.2 GPa in the AUK and 9.6 GPa in the ADK. The appearance of a 1-2 GPa interval of clinopyroxene as liquidus phase between the olivine and the garnet portions in both of the compositions, combined with the assumption that olivine was a residual phase during komatiite melting, indicates that garnet is not a residual phase following the melt separation of either the AUK or the ADK. Assuming that both of the komatiites represent near primary melts, I favour melting under the conditions of the olivine-clinopyroxene cosaturation points corresponding to 160 and 300 km depth for the AUK and ADK, respectively.

Small amounts of garnet originally present in the source peridotites were likely consumed by the estimated 10-30 % melting to form these komatiites. The Al-depleted signature of the komatiite formed at about 9.6 GPa is ascribed to garnet fractionation in a rising diapir prior to melt separation. The pressure of ADK melt separation from the peridotite source may mark a density crossover between olivine and komatiitic melts.

Table 1 General Features of Al-undepleted and Al-depleted komatiites and Compositions of Starting Materials

Oxides (wt%)	M620*	HSS-15*	AUK*[a]	ADK*[b]	Pyrolite[c]	KLB-1[d]	C1[e]
SiO_2	45.60	46.77	45.90	47.16	45.20	44.48	33.64
TiO_2	0.40	0.33	0.41	0.38	0.71	0.16	0.11
Al_2O_3	7.95	3.42	7.97	4.09	3.54	3.59	2.42
FeO(t)	12.66	11.26	11.07	12.01	8.47	8.10	36.20
MnO	0.20	0.19	0.21	0.20	0.14	0.12	0.38
MgO	25.00	31.51	26.38	27.97	37.48	39.22	24.23
CaO	7.60	5.67	7.74	6.61	3.08	3.44	1.92
Na_2O	0.01	0.12	0.43	0.37	0.57	0.30	1.00
K_2O	0.02	0.08	0.09	0.04	0.13	0.02	0.10
Mg #	77.9	83.3	80.9	80.6	88.8	89.6	54.4
CaO/Al_2O_3	0.96	1.66	0.97	1.62	0.87	0.96	0.79
Al_2O_3/TiO_2	19.9	10.4	19.4	10.8	4.99	22.4	22.0
(La/Sm)n			0.4-0.8[f]	~1[f]			1
(Gd/Yb)n			~1[f]	~1.43[f]			1
Zr/Y			2.5[f]	2.8-4.6[f]			2.5
Ti/Zr			110[f]	100[f]			111
Ti/Sc			79[f]	110[f]			75

Note: AUK=Al-undepleted komatiite; ADK=Al-depleted komatiite; C1= mean C1 chondrite; Mg#=[Mg/(Mg+Fe)] x100. *:-Analyses normorlized to 100% on a volatile free basis. Source: M620: Arndt and Nesbitt (1984); HSS-15: Smith and Erlank (1982); **a:** average of 22 samples from Nesbitt et al.(1979); Arndt and Nesbitt (1984); Cattell and Arndt (1987) and Nisbet et al. (1987); **b:** average of 18 samples from Nesbitt et al. (1979) and Smith and Erlank (1982); **c:** Ringwood (1966); **d:** peridotite (Takahashi, 1986); **e:** calculated oxides normalized to 100 % from the atomic abundances of Anders and Grevesse (1989), **f:** Nesbitt et al.(1982).

Table 2 Experimental Conditions and Results

	Run#	P (GPa)	T* (°C)	Time (min.)	Heater	Container	Result AUK(M620)	Result ADK(HSS-15)
1	206	4.0	1600	25	B	C	ol+cpx+ga	ol+cpx+ga
2	202	4.0	1650	65	B	C	ol+cpx+ga+l	ol+cpx+ga+l
3	138	4.0	1700	5	A	C	ol+cpx+l	ol+cpx+l
4	234	4.0	1780	10	B	C	l	l
5	212	5.0	1700	60	B	C	ol+cpx+ga+l	ol+cpx+ga+l
6	236	5.0	1750	10	B	C	ol+cpx+l	ol+cpx+l
7	135	5.0	1770	5	A	C	ol+l	ol+l
8	218	5.0	1800	5	B	C	l	l
9	260	5.5	1780	5	B	C	ol+cpx+l	
10	197	6.0	1700	26	B	C	ol+cpx+ga	ol+cpx+ga
11	220	6.0	1750	30	B	C	ol+cpx+ga+l	ol+cpx+ga+l
12	168	6.0	1800	10	B	C	cpx+ga+l	ol+l
13	189	6.0	1820	10	B	C	cpx+l	ol+l
14	192	6.0	1850	20	B	C	l	l
15	225	7.0	1750	13	B	C	ol+cpx+ga+l	ol+cpx+ga
16	136	7.0	1780	4	A	C	ol+cpx+ga+l	ol+cpx+ga+l
17	270	7.0	1810	5	B	C	cpx+ga+l	
18	156	7.0	1830	7	B	C	ga+l	ol+l
19	127	7.0	1850	1.5	A	C	l	l
20	227	9.0	1790	8	B	Mo	ol+cpx+ga	ol+cpx+ga
21	244	9.0	1820	5	B	Mo	ol+cpx+ga+l	ol+cpx+ga+l
22	263	9.0	1835	5	B	Mo	cpx+ga+l	
23	152	9.0	1860	6	B	C	ga+l	ol+l
24	257	10.0	1800	6	B	Mo	ol+cpx+ga+l	ol+cpx+ga
25	247	10.0	1860	5	B	Mo	ga+l	ol+cpx+l
26	275	11.0	1875	4	B	Mo		cpx+l
27	245	12.0	1800	5	B	C	ol+cpx+ga	ol+cpx+ga
28	242	12.0	1900	5	B	Mo	l	ga+l

Note: **A**: simple cylindrical heater; **B**: sectioned heater (see text); **C**: graphite; **Mo**: molybdenum; **ol**: olivine; **cpx**: clinopyroxene; **ga**: garnet; **l**: quenched liquid.
*: thermocouple reading

Table 3 Microprobe Analyses of Olivines in Experimental Runs (wt %)

Sample	M620	M620	HSS-15	HSS-15	HSS-15	HSS-15	HSS-15
Run#	138	260	138	135	168	156	247
P (GPa)	4	5.5	4	5	6	7	10
T (°C)	1700	1780	1700	1770	1800	1830	1860
SiO_2	39.4 (0.24)	40.0 (0.32)	39.3 (0.14)	40.4 (0.04)	41.2 (0.30)	40.9 (1.28)	40.9 (0.48)
Al_2C_3	0.16 (0.01)	0.83 (0.13)	0.14 (0.04)	0.23 (0.04)	0.12 (0.03)	0.17 (0.17)	0.82 (0.13)
FeO(t)	10.2 (0.08)	9.97 (1.21)	10.9 (0.09)	10.0 (0.01)	7.15 (0.15)	7.82 (0.14)	9.97 (0.57)
MnO	0.12 (0.02)	0.11 (0.04)	0.17 (0.01)	0.13 (0.02)	0.11 (0.02)	0.12 (0.02)	0.15 (0.03)
MgO	49.0 (0.04)	49.2 (0.69)	47.3 (0.06)	49.2 (0.09)	52.6 (0.19)	51.0 (1.04)	47.6 (0.12)
CaO	0.33 (0.01)	0.31 (0.14)	0.35 (0.02)	0.33 (0.01)	0.22 (0.01)	0.33 (0.14)	0.78 (0.38)
Total	99.21	100.42	98.16	100.29	101.40	100.34	100.22
Fo*	89.4	89.7	88.4	89.6	92.8	92.0	89.3
Kd**	0.41	0.40	0.65	0.57	0.38	0.43	0.59
			Formula based on 4 oxygen atoms				
Si	0.978	0.979	0.988	0.983	0.986	0.990	0.999
Al	0.005	0.002	0.007	0.004	0.003	0.005	0.002
Fe	0.212	0.204	0.205	0.249	0.143	0.158	0.204
Mn	0.003	0.002	0.003	0.004	0.002	0.003	0.003
Mg	1.813	1.791	1.796	1.764	1.873	1.842	1.735
Ca	0.009	0.008	0.009	0.009	0.006	0.009	0.020
Total	3.020	2.986	3.008	3.013	3.013	3.007	2.963

* Fo=[Mg/(Fe(t)+Mn+Mg)]X100; ** Kd=[$(FeO(t)/MgO)^{olivine}$/$(FeO(t)/MgO)^{bulk\ komatiite}$]

Note: numbers in brackets represent the uncertainty of analyses.

Table 4 Microprobe Analyses of Clinopyroxenes and Garnets in Experimental Runs (wt%)

Sample	M620	HSS-15	HSS-15	HSS-15	M620	HSS-15
Run#	260	138	247	275	247	242
P (GPa)	5.5	4	10	11	10	12
T (°C)	1780	1700	1860	1875	1860	1900
Mineral	cpx	cpx	cpx	cpx	ga	ga
SiO_2	52.7 (0.24)	54.2 (0.31)	55.3 (0.40)	57.5 (0.34)	43.5 (0.43)	45.5 (0.56)
TiO_2	0.16 (0.01)	0.06 (0.01)	0.08 (0.03)	0.02 (0.01)	0.25 (0.03)	0.14 (0.02)
Al_2O_3	5.68 (0.12)	2.46 (0.11)	1.43 (0.52)	2.25 (0.55)	21.7 (0.24)	20.2 (0.22)
FeO(t)	7.95 (0.33)	7.63 (0.09)	7.14 (0.35)	3.74 (0.16)	5.90 (0.12)	5.13 (0.17)
MnO	0.16 (0.01)	0.15 (0.02)	0.18 (0.03)	0.15 (0.02)	0.19 (0.02)	0.16 (0.01)
MgO	26.8 (0.76)	32.7 (0.23)	26.1 (0.74)	30.8 (0.89)	23.8 (0.38)	25.1 (0.35)
CaO	6.75 (0.21)	2.56 (0.02)	9.82 (0.64)	6.58 (0.12)	4.13 (0.17)	4.29 (0.09)
Na_2O	0.03 (0.01)	0.04 (0.01)	0.27 (0.03)	0.23 (0.02)		
Total	100.23	99.80	100.32	101.27	99.47	100.52
	Formula based on 6 oxygen atoms				Formula based on 12 oxygen atoms	
Si	1.864	1.904	1.963	1.966	3.057	3.150
Ti	0.004	0.002	0.002	0.001	0.013	0.007
Al	0.237	0.102	0.060	0.091	1.798	1.648
Fe	0.235	0.224	0.212	0.107	0.347	0.297
Mn	0.005	0.005	0.005	0.004	0.011	0.009
Mg	1.413	1.708	1.380	1.570	2.493	2.590
Ca	0.256	0.096	0.374	0.241	0.311	0.318
Na	0.002	0.003	0.019	0.015		
Total	4.016	4.044	4.015	3.995	8.030	8.019
En	74.2	84.2	70.2	81.9	Py 79.1	80.8
Fs	12.3	11.1	11.8	5.6	Alm 11.0	9.3
Wo	13.5	4.7	19.0	12.5	Gr 9.9	9.9
DAl*	0.71	0.72	0.42	0.66	2.73	5.91
DCa**	0.89	0.45	1.73	1.16	0.54	0.76

*: $DAl=[(Al_2O_3)^{\text{liquidus phase}}/(Al_2O_3)^{\text{bulk komatiite}}]$; **: $DCa=[(CaO)^{\text{liquidus phase}}/(CaO)^{\text{bulk komatiite}}]$

Numbers in brackets represent the uncertainty of analyses.

Figure 1: Weight percent oxide variation diagrams for representative samples of Al-undepleted komatiites (AUK) and Al-depleted komatiites (ADK)

Solid squares: komatiites, upper diagrams (AUK): from Munro Township, Ontario (Arndt and Nesbitt, 1984; Arndt et al., 1977; Nesbitt et al.,1979), Newton Township, Ontario (Cattell and Arndt, 1987), Belingwe greenstone belt, Zimbabwe (Nisbet et al., 1987); lower diagrams (ADK): from Barberton Mountain Land, South Africa (Nesbitt et al., 1979; Smith and Erlank, 1982). **Solid diamonds**: starting material compositions (see Table 1), AUK: M620, ADK: HSS-15. **Solid triangles**: peridotite compositions (see Table 1), pyrolite and KLB-1. **Open squares**: liquidus olivine compositions (see Table 3), AUK: runs 138 and 260, ADK: runs 138, 135, 168, 156 and 247. **Open circles**: liquidus clinopyroxene compositions (see Table 4), AUK: run 260, ADK: runs 38, 247 and 275. **Open triangles**: liquidus garnet compositions (Table 4), AUK: run 247, ADK: run 242. The lines are least squares regression fit to the komatiite composition only.

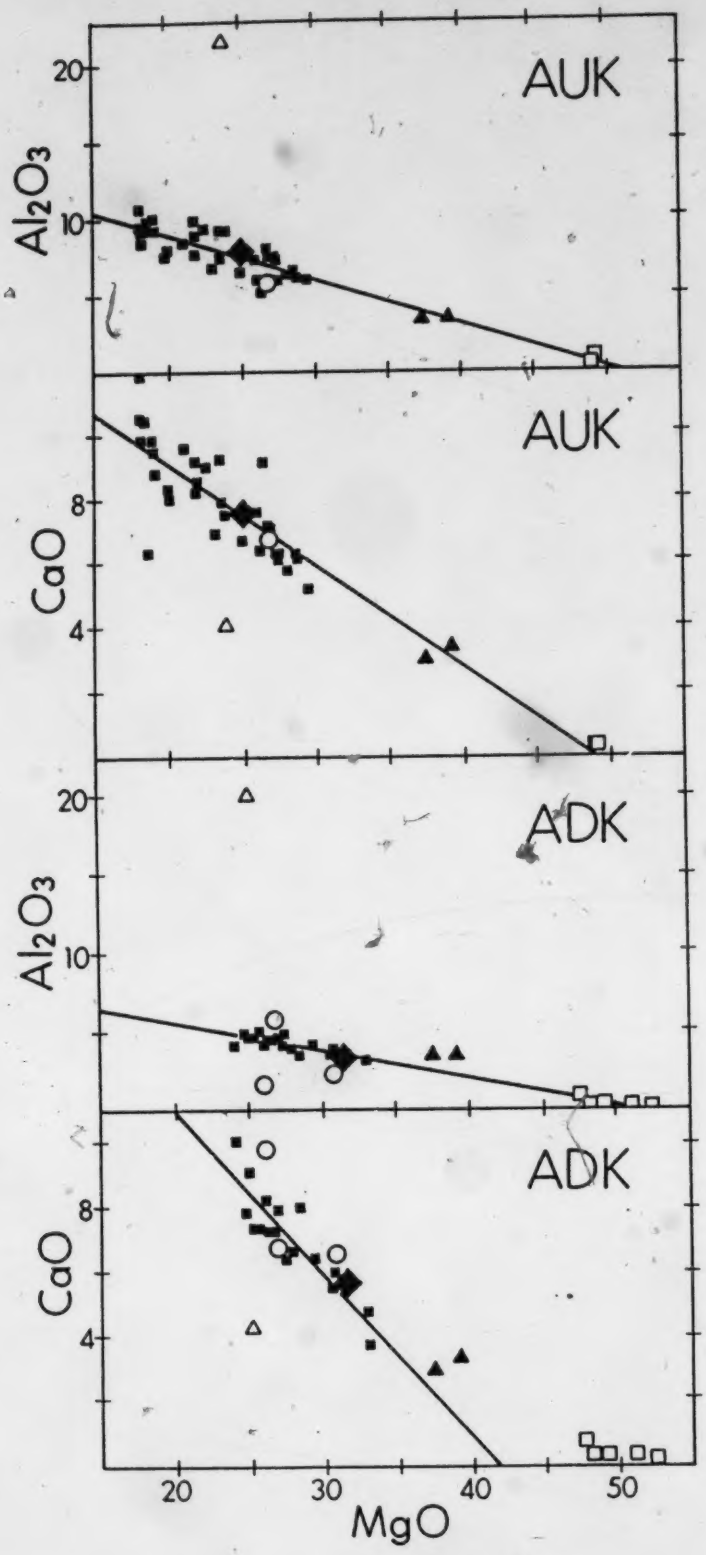
AUK
Al_2O_3
20
10
AUK
CaO
8
4
ADK
Al_2O_3
20
10
ADK
CaO
8
4
20
30
40
50
MgO

Figure 1

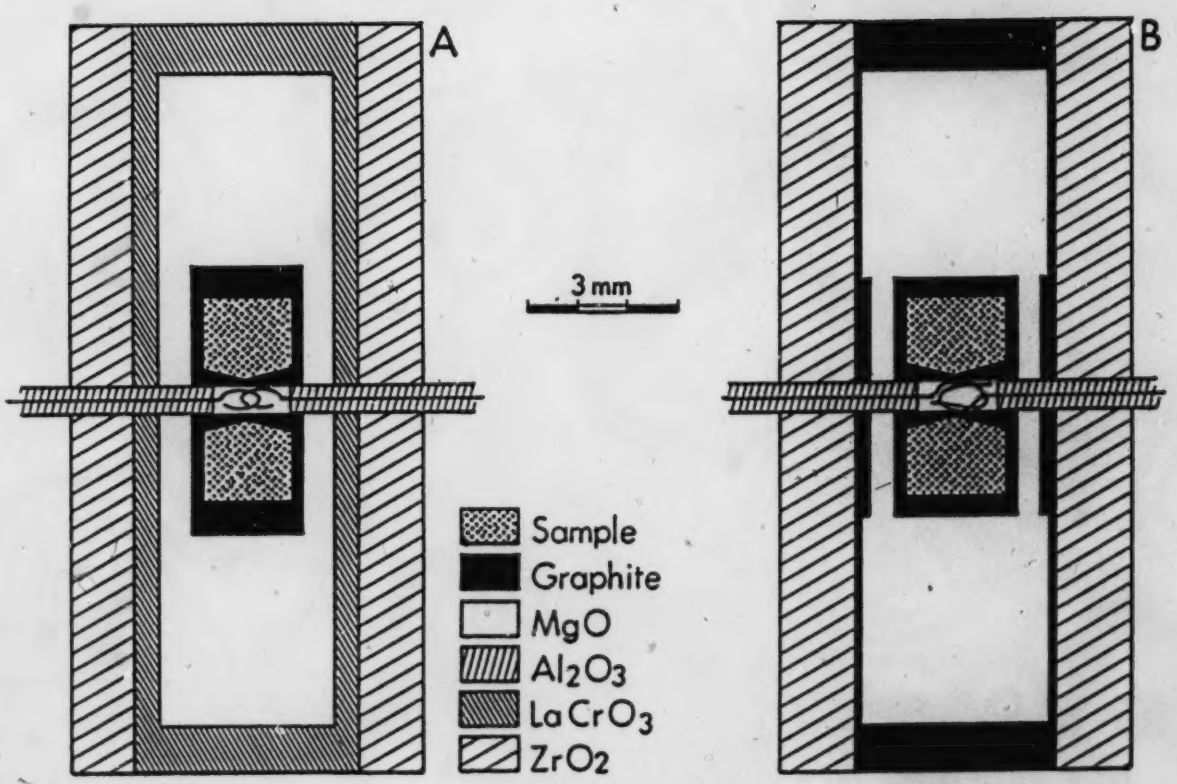

Figure 2 Cross section of the furnace assemblies

A: Simple cylindrial furnace. B: Sectioned furnace. The experiments were also carried out using simple cylindrical graphite heaters and sectioned $LaCrO_3$ heaters.

Figure 3 Back scattered electron SEM photomicrographs of run products

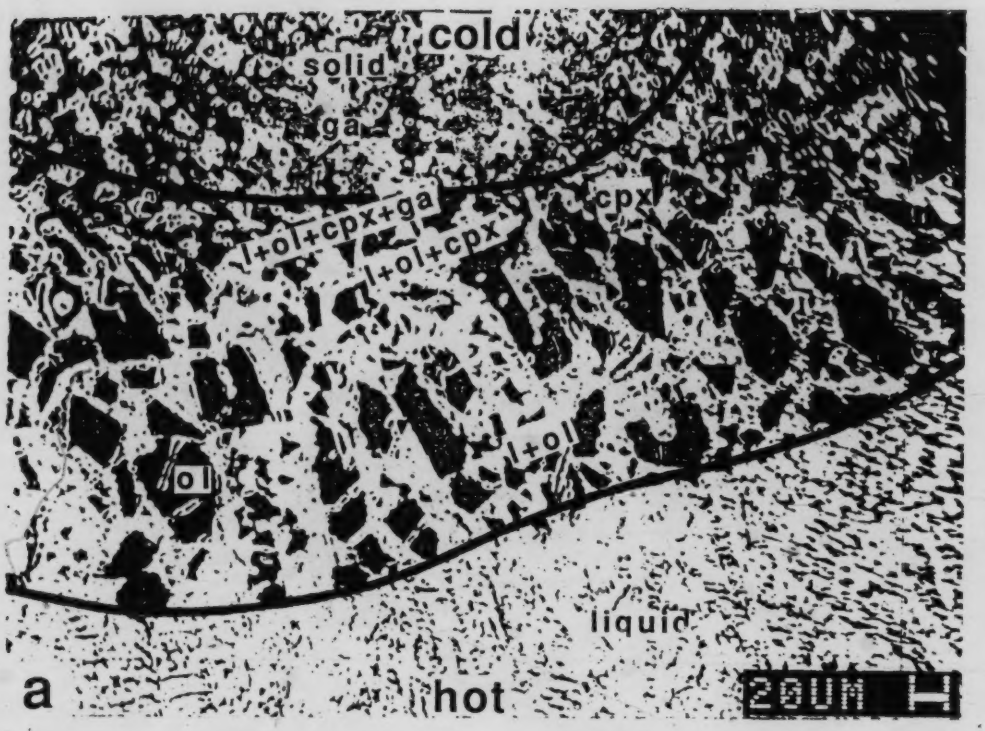

(a) (run 135, HSS-15): Distribution of the zones of quenched liquid, quenched liquidus+solids and only solids in a run product from an experiment using a simple cylindrical heater (Figure 2A). The lower line is the liquidus and the upper line is the solidus. l and liquid: quenched liquid, ol: olivine, cpx: clinopyroxene, ga: garnet. l+ol+cpx marks the location of the first clinopyroxene appearance and l+ol+cpx+ga marks the location of the first garnet appearance with increasing distance from the hot end of the sample.

b

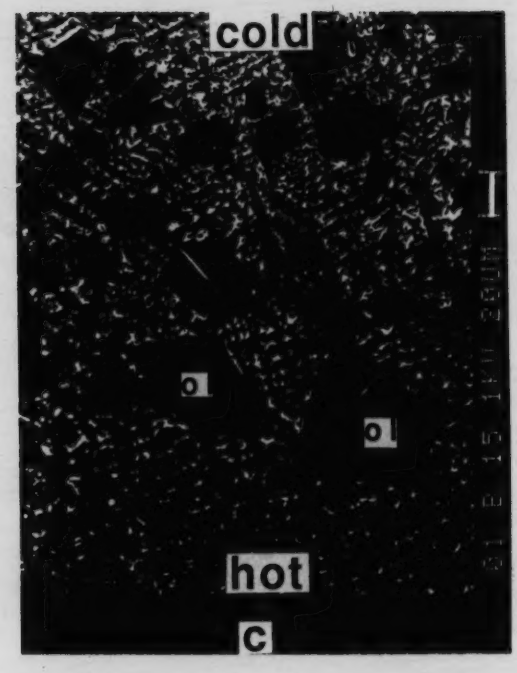

c

(b) (run 245, a mixture of pure enstatite and diopside): equilibrium intergowth texture of orthopyroxene (opx) and clinopyroxene (cpx) from a 210 minute long experiment at 7 GPa, 1500 °C, using a sectioned furnace (Figure 2 B).

(c) (run 156, HSS-15): coarse, euhedral and unzoned liquidus olivines.

Figure 3

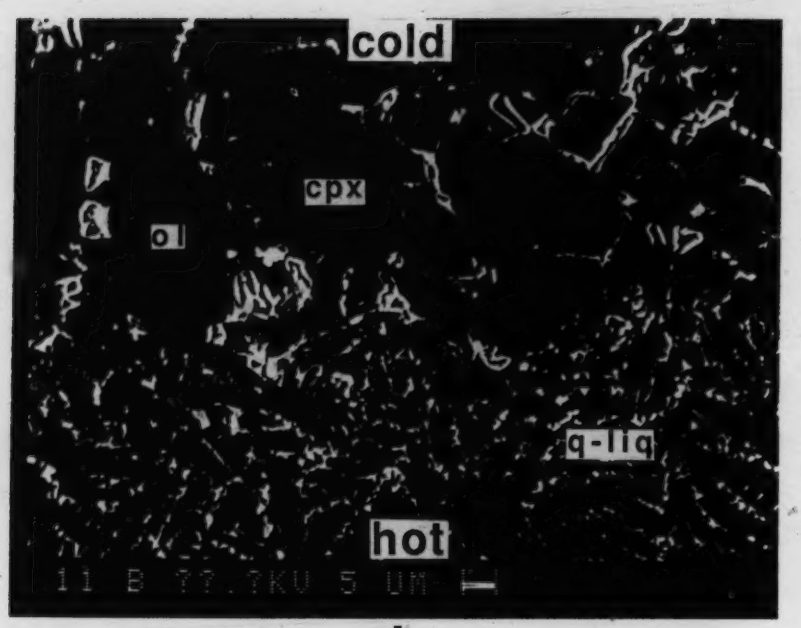

d

Figure 3

(**d**) (run 260, m620): coarse, euhedral and unzoned olivines (ol) and clinopyroxenes (cpx) coexist with liquid (q-liq).

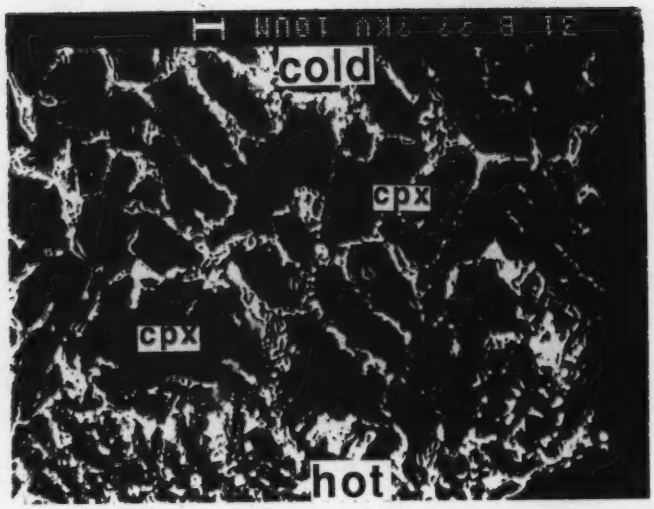

e

Figure 3

(e) (run 275, HSS-15): coarse, unzoned clinopyroxene (cpx) in equilibrium with a liquid (q-liq)

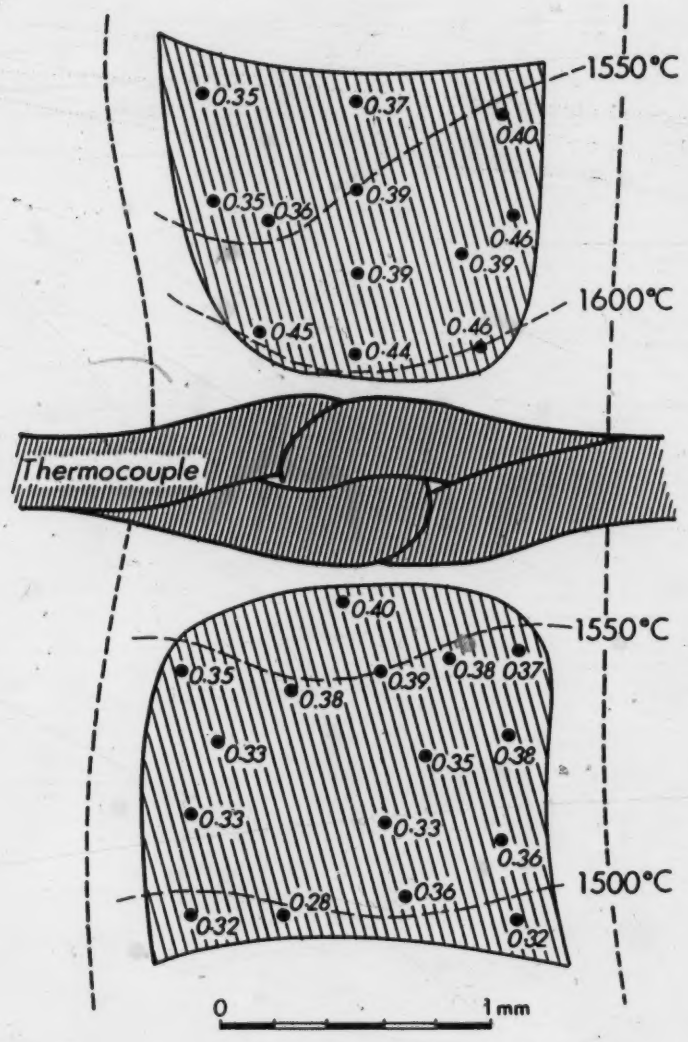

Figure 4 Temperature distribution within two-pyroxene charges from an experiment at 1500 °C (Thermocouple reading) and 7 GPa using a sectioned graphite heater (Figure 2B)

The numbers shows the locations of two coexisting pyroxenes and their $K_d(1-X_{Ca})^{cpx}/(1-X_{Ca})^{opx}$. Light stippled lines indicate temperature contours, and heavy stippled lines are the outside walls of the graphite capsules. See text and Figure 3b for further explanations.

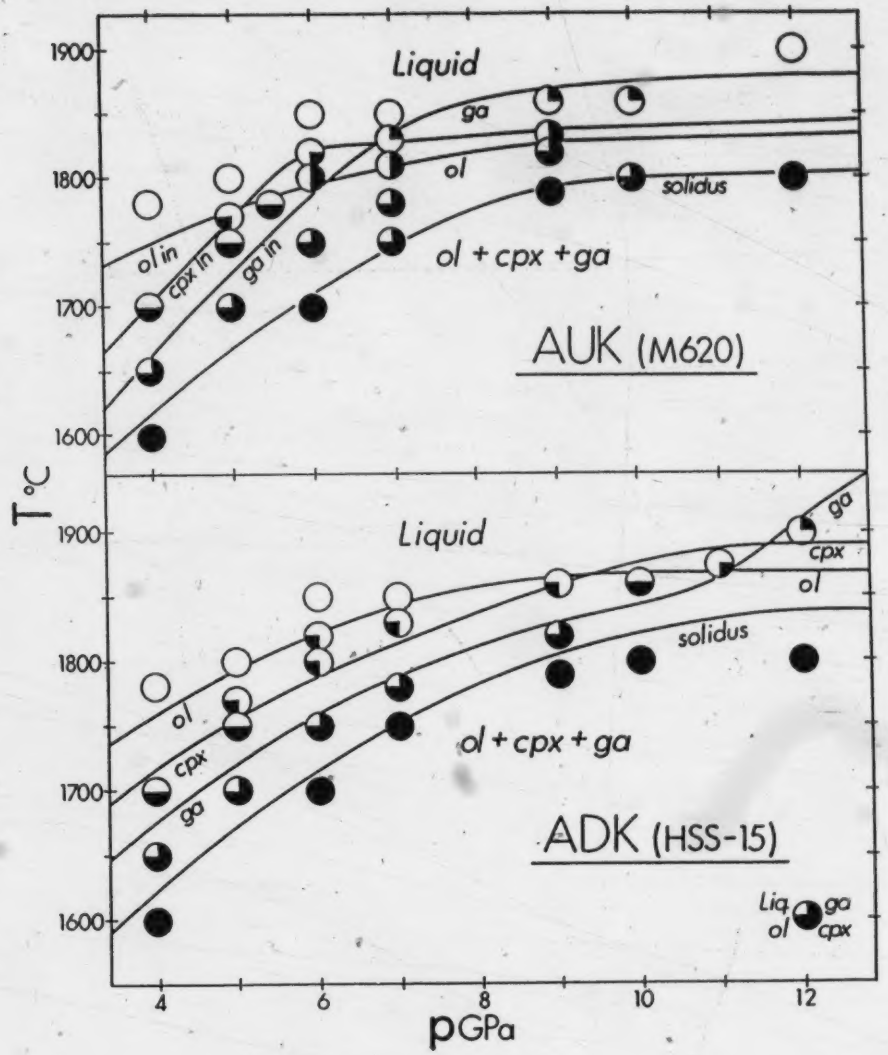

Figure 5 Phase diagrams of the Al-undepleted (AUK) and Al-depleted (ADK) komatiites (samples M620 and HSS-15, respectively).

The curved lines indicate the disappearance of the phases olivine (ol), clinopyroxene (cpx) and garnet (ga) with increasing temperature and melt fraction.

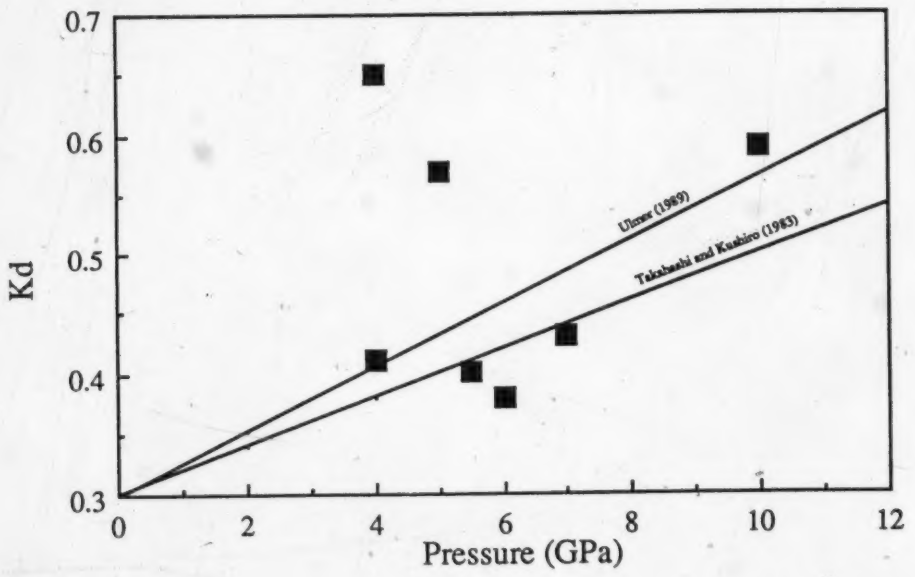

Figure 6 Distribution coefficient ($K_{d(Fe/Mg)^{(ol/bulk\ komatiite)}}$) of Fe/Mg between liquidus olivine and bulk komatiite as a function of pressure

Solid squares: Data from this study. The line are calculated from the regression equations of Ulmer(1989) and Takahashi and Kushiro (1983).

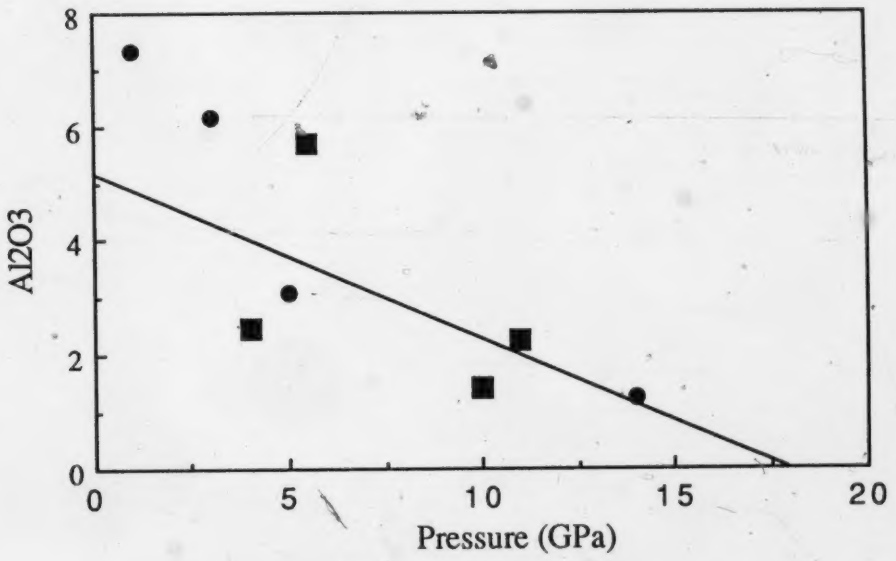

Figure 7 Al_2O_3 content of the clinopyroxene as a function of pressure

Solid squares: Data of this study (Table 4); Solid circles: Takahashi (1986). The regression line is based on the 4 solid square data points.

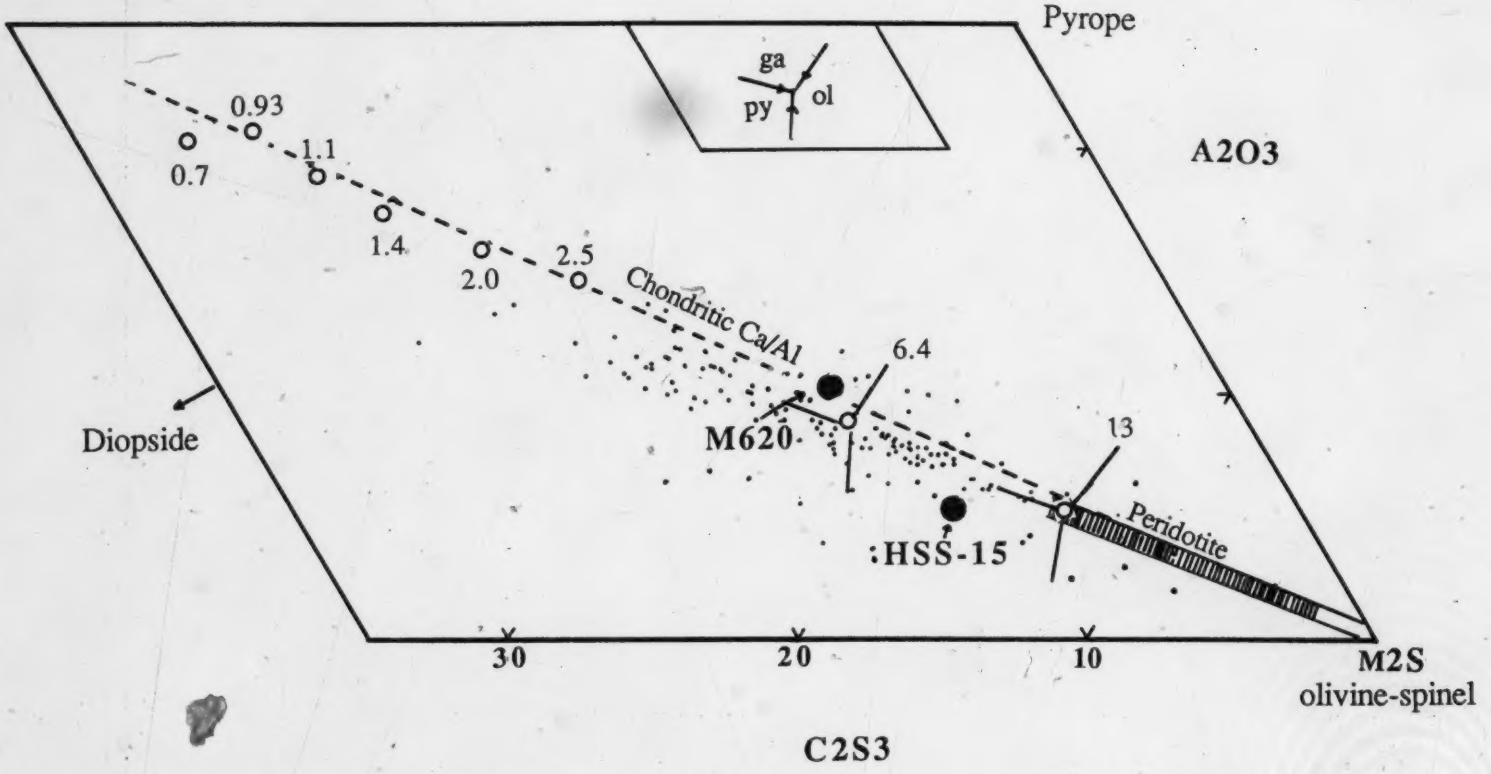

Figure 8 Komatiite compositions projected from enstatite (MS) onto the plane M_2 C_2S_3-A_2S_3 in the system CMAS (CaO-MgO-Al_2O_3-SiO_2)

Projected method of O'Hara(1968). The data points are the same as in Herzberg and Ohtani (1988). Small dots: komatiites; Rings: pseudoinvariant points at pressures of 0.7 to 13 GPa; Large dots: Starting materials.

Figure 9 Schematic diapir model for the origin of Al-undepleted and Al-depleted komatiites

The peridotite solidus and liquidus are from Herzberg et al. (1989). The lines marked 1° and 2° represent adiabatic gradients for rising peridotite diapirs of 1 °C/kbar and 2 °C/ kbar, respectively. The arrows indicate the separation of the AUK and ADK liquids from the source. A possible density crossover is indicated at about 300 km ($\rho_{peridotite} = \rho_{komatiitic\ liquid}$) at which the density of an ultramafic liquid is close to that of olivine. Garnet is the only phase denser than the liquid between 300 and 400 km depths. Al-depleted komatiites were formed by partial melting of a peridotitic diapir which started to melt at depth greater than that of the density crossover, whereas Al-undepleted komatiite were formed by partial melting of a peridotitic diapir starting to melt above the density crossover.

The garnet fractionation from the rising ADK-diapir is facilitated by:

1. The high density of the ultramafic liquid below about 300 km;

2. The near coincidence of the adiabatic path (1-2 °C/kbar) and the peridotite solidus.

These factors prevent efficient melt separation from the rising diapir below about 300 km depth. The adiabatic path of the AUK-diapir intersects the solidus at a greater angle than that of the ADK-diapir.

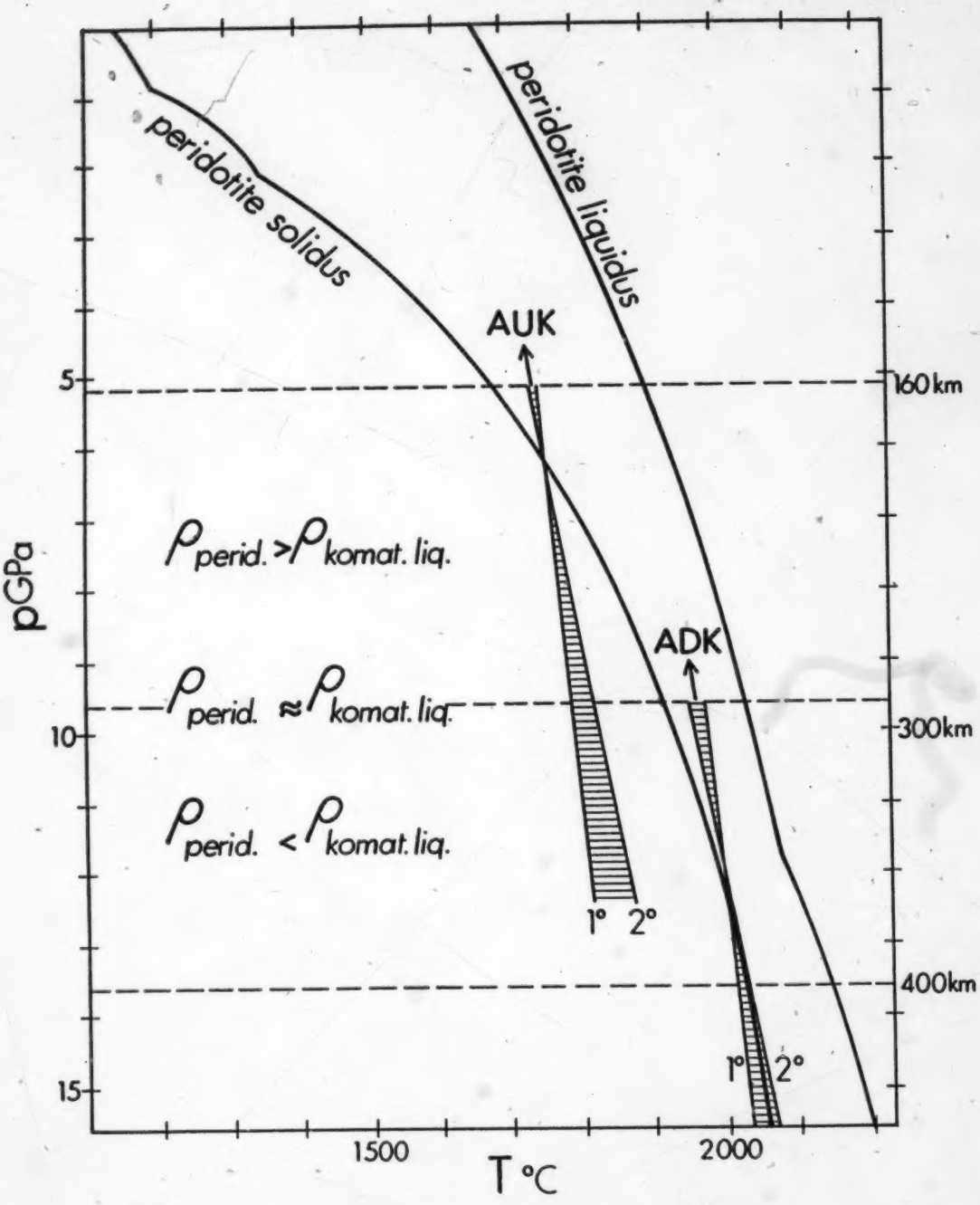
peridotite solidus
peridotite liquidus
AUK
ADK
5
10
15
pGPa
160km
300km
400km
$\rho_{perid.} > \rho_{komat.\,liq.}$
$\rho_{perid.} \approx \rho_{komat.\,liq.}$
$\rho_{perid.} < \rho_{komat.\,liq.}$
1° 2°
1° 2°
1500
2000
T °C

Figure 9

VII. References

Agee, C. B., and D. Walker, Static composition and olivine flotation in ultrabasic liquid, J. Geophys. Res., 93, 3437-3449, 1988.

Albee, A. L., and L. Ray, Correction factors for electron microprobe micro analyses of silicates, oxides, carbonates, phosphates and sulfates, Anal. Chem., 42, 1408-1414, 1970.

Anders, E., and N. Grevesse, Abundances of the elements: meteoric and solar, Geochim. Cosmochim. Acta, 53, 197-214, 1989.

Anderson, D. L., Theory of the Earth, Blackwell, Boston, 1989.

Anhaeosser, C. R., The evolution of the early precambrian crust of the Southern Africa, Philos. Trans. R. Soc. Lond. A, 273, 359-388, 1973.

Anhaeusser, C. R., The geological evolution of primitive earth-evidence from the Barberton Mountain Land, in Evolution of the Earth' s crust, edited by D. H. Tarling, pp 71-106, Academic Press, London, 1978.

Anhaeusser, C. R., C. Riering, M. J. Viljoen, and R. P. Viljoen, The Barberton Mountain Land: a model of the elements and evolution of an Archaean fold belt, Trans. Geol. Soc. S. Afr., 71 (annex), 225-253, 1968.

Arndt, N. T., Melting relations of ultramafic lavas (komatiites) at 1 atm and high pressure, Carnegie Inst. Wash. Yearb., 75, 555-562, 1976.

Arndt, N. T., Ultrabasic magmas and high-degree melting of the mantle, Contrib. Mineral. Petrol., 64, 205-221, 1977.

Arndt, N. T., The field characteristics and petrology of Archean and proterozoic komatiites, Can. Mineral., 17, 147-163, 1979.

Arndt, N. T., A. J. Naldrett, and D. R. Pyke, Komatiitic and iron-rich tholeiitic lavas in Munro Township, northeast Ontario, J. Petrol.,18, 319-369, 1977.

Arndt, N. T., and R. W. Nesbitt, Geochemistry of Munro Township basalts. In Komatiites, edited by N. T. Arndt and E. G. Nisbet, pp 309-330, George Allen and Unwin, London,1982.

Arndt, N. T., and R. W. Nesbitt, Magma mixing in komatiitic lavas from Munro Township, Ontario, In Archaean Geochemistry, edited by Kroner et al., pp 99-114, Springer-Verlag, 1984.

Arth, J. G., N. T. Arndt, and A. J. Naldrett, Genesis of Archean komatiites from Munro Township,Ontario: trace element evidence from northeast , Geology (Boulder), 5, 590-594, 1977.

Bence, A. E., and A. L. Albee, Empirical correction factors for the electron microanalysis of silicates and oxides, J. Geol., 76, 382-403, 1968.

Bickle, M. J., C. E. Ford, and E. G. Nisbet, The petrogenesis of peridotitic komatiites: evidence from high-pressure melting experiments, Earth Planet. Sci. Lett., 37, 97-106, 1977.

Biggar, G. M., Molybdenum as a container for melts containing iron oxide, Amer. Ceram. Soc. Bull., 49, 286-288, 1970.

Boyd, F. R., and J. L. England, The quartz-coesite transition, J. Geophys. Res., 65, 749-756, 1960.

Cattell, A., and N. T. Arndt, Low- and high-alumina komatiites from a late Archaean sequence, Newton Township, Ontario, Contrib. Mineral. Petrol., 97, 218-227, 1987.

Cawthorn, R. G., and D. F. Strong, The petrogenesis of komatiites and related rocks as evidence for a layered upper mantle, Earth Planet. Sci. Lett., 23, 369-375, 1974.

Fujii, T., M. Tachikara, and K. Kurita, Melting experiments in the system CaO-MgO-Al_2O_3-SiO_2 to 8 GPa: constraints on the origin of komatiites, submitted to J. Geophys. Res., 1989.

Getting, I. C., and G. C. Kennedy, Effect of pressure on the emf of chromel-alumel and platinum-platinum 10% Rhodium thermocouples, J. Ap. lied. Phys., 41, 4552-4562, 1970.

Green, D. H., Genesis of Archaean peridotitic magma and constraints on Archaean geothermal gradients and tectonics, Geology (Boulder), 3, 15-18, 1975.

Green, D. H., I. A. Nicholls, M. J. Viljoen, and R. P. Viljoen, Experimental demonstration of the existence of peridotitic liquids in earliest Archaean magmatism, Geology (Boulder), 3, 11-15, 1975.

Green, D. H., and A. E. Ringwood, The genesis of basaltic magmas, Contrib. Mineral. Petro.,15, 103-190, 1967.

Hall, H. T., Fixed points near room temperature, In Accurate characterization of the high-pressure environment, edited by E. C. Lloyd, NBS Spec. Publ., 326, 313-314, 1971.

Hamilton, P. J., N. M. Evensen, R. K. O'nions, H. S. Smith, and A. J. Erlank, Sm-Nd dating of Onverwacht group volcanics, southern Africa, Nature., 279, 298-300, 1979.

Herzberg, C. T., Solidus and liquidus temperatures and mineralogies for anhydrous garnet-lherzolite to 15 GPa, Phys. Earth Planet. Inter., 32, 193-202, 1983.

Herzberg, C. T., Magma density at high pressure, Part 1: The effect of composition on the elastic properties of silicate liquids, In Magmatic processes: Physiochemical processes, edited by B. O. Mysen, Geochem. Soc. Spec. Publ., 1, 25-46, 1987a.

Herzberg, C. T., Magma density at high pressure, Part 2: A test of the olivine flotation hypothesis, In Magmatic processes: Physiochemical processes, edited by B. O. Mysen, Geochem. Soc. Spec. Publ.,1, 47-58,1987b.

Herzberg, C. T., T. Gasparik, and H. Sawamoto, Origin of mantle peridotite: constraints from melting experiments to 15 GPa, Submitted to J. Geophys. Res., 1989.

Herzberg, C. T., and M. J. O'Hara, Origin of mantle peridotite and komatiite by partial melting, Geophys. Res. Lett., 12, 541-544, 1985.

Herzberg, C. T., and E. Ohtani, Origin of komatiite at high pressures, Earth Planet. Sci. Lett., 88, 321-329, 1988.

Homan, C. G., Phase diagram of Bi up to 140 kbars, J. Phys. Chem. Solids, 36, 1249-1254, 1975.

Irvine, T. N., and M. R.Sharp, Source-rock compositions and depths of origin of Bushveld and Stillwater magmas. Carnegie Inst. Wash. Yearb., 81, 294-303, 1982.

Ito, E., and E. Takahashi, Ultrahigh pressure phase transformations and the constitution of deep mantle, in High pressure research in mineral physics, edited by M. H. Manghnani and Y. Syono, pp 221-229, Terrapub Tokyo,1987.

Ito, E., E. Takahashi, and Y. Matsui, The mineralogy and chemistry of the lower mantle: an implication of the ultrahigh-pressure phase relations in the system MgO-FeO-SiO_2, Earth Planet. Sci. Lett., 67, 238-248, 1984.

Jahn, B. M., B. Auvray, S. Blais, R. Capdevila, J. Cornichet, F. Vidal, and J. Hameurt, Trace element geochemistry and petrogenesis of Finnish greenstone belts, J. Petrol., 21, 201-204, 1980.

Jahn, B. M., G. Gruau, and A. Y. Glikson, Komatiites of the Onverwacht Group, S. Africa: REE geochemistry, Sm/Nd age and Mantle evolution, Contrib. Mineral. Petrol., 80, 25-40, 1982.

Kanzaki, M., Ultrahigh-pressure phase relations in the system $Mg_4Si_4O_{12}$-$Mg_3Al_2Si_3O_{12}$, Phys. Earth Planet. Inter., 49, 168-175, 1987.

Kushiro, I., A new furnace assembly with a small temperature gradient in solid-media, high-pressure apparatus, Carnegie Inst. Wash. Yearb., 75, 832-833, 1976.

Lesher, C. E., and D. Walker, Cumulate compaction and melt migration in a temperature gradient, J. Geophys. Res., 93, 10295-10311, 1988.

McCall, G. J. H., and J. Leishman, Clues to the origin of Archaean engesynclinal peridotites and the nature of serpentinisation, Geol. Soc. Aust. Sp. Publ., 3, 281-300, 1971.

Mirwald, P. W., and H. J. Massonne, The low-high quartz and quartz-coesite transition to 40 kbar between 600 °C and 1600 °C and some reconnaissance data on the effect of $NaAlO_2$ component on the low quartz-coesite transition, J. Geophys. Res., 85, 6983-6990, 1980.

Nesbitt, R. W., B. M. Jahn, and A. C. Purvis, Komatiites: an early precambrian phenomenon, J. Volcanol. Geothermal. Res., 14, 31-45, 1982.

Nesbitt, R. W., S. S. Sun, and A. C. Purvis, Komatiites: geochemistry and genesis, Can. Mineral., 17, 165-186, 1979.

Nickel, K. G., and G. Brey, Subsolidus orthopyroxene-clinopyroxene systematics in the system CaO-MgO-SiO_2 to 60 kb: a reevaluation of the regular solution model, Contrib. Mineral. Petrol., 87, 35-42, 1984.

Nickel, K. G., G. P. Brey, and L. Kogarko, Orthopyroxene-clinopyroxene equilibira in the system CaO-MgO-Al_2O_3-SiO_2 (CMAS): new experimental results and implications for two-pyroxene thermometry, Contrib. Mineral. Petrol., 91, 44-53, 1985.

Nisbet, E. G., The tectonic setting and petrogenesis of komatiites, in Komatiites, edited by N. T. Arndt and E. G. Nisbet, pp 501-520, George Allen and Unwin, London, 1982.

Nisbet, E. G., N. T. Arndt, M. J. Bickle, W. E. Cameron, C. Chauvel, M. Cheadle, E. Hegner, T. K. Kyser, A. Martin, R. Renner, and E. Roedder, Uniquely fresh 2.7 Ga komatiites from the Belingwe greenstone belt, Zimbabwe, Geology (boulder), 15, 1147-1150, 1987.

Nisbet, E. G., and D. Walker, Komatiites and the structure of the Archaean mantle, Earth Planet. Sci. Lett., 60, 105-113, 1982.

O'Hara, M. J., The bearing of phase equilibria studies in synthetic and natural systems on the origin and evolution of basic and ultrabasic rocks, Earth Sci. Rev., 4, 69-113, 1968.

O'Hara, M. J., M. J. Sauders, E. P. L. Mercy, Garnet-peridotite primary ultrabasic magma and eclogites; Interpretation of upper mantle processes in Kimberlite, Phys. Chem. Earth, 9, 571-604, 1975.

Ohtani, E., Generation of komatiite magma and gravitational differentiation in the deep upper mantle, Earth Planet. Sci. Lett., 67, 261-272, 1984.

Ohtani, E., Chemical stratification of the mantle formed by melting in the early stage of the terrestrial evolution, Tectonophys., 154, 201-210, 1988.

Ohtani, E., T. Kato, and H. Sawamoto, Melting of a model chondritic mantle to 20 GPa, Nature, 322, 1986.

Pyke, D. R., A. J. Naldrett, and O. R. Eckstrand, Archean ultramafic flows in Munro Township, Ontario, Geol. Soc. Am. Bull., 84, 955-978, 1973.

Ringwood, A. E., Mineralogy of the mantle, In Advances in Earth Sciences, edited by P. M. Hurley, pp 357-399, MIT press, Cambridge, Mass, 1966.

Ringwood, A. E., Composition and petrology of the Earth's mantle, pp 24-122, McGraw-Hill, New York, 1975.

Scarfe, C. M., and E. Takahashi, Melting of garnet peridotite to 13 GPa and the early history of the upper mantle, Nature, 322, 354-356,1986.

Smith, H. S., and A. J. Erlank, Geochemistry and petrogenesis of komatiites from the Barberton greenstone belt, South Africa, In Komatiites, edited by N. T. Arndt and E. G. Nisbet, pp 347-397, George Allen and Unwin, London,1982.

Suito, K., Phase relation of pure Mg_2SiO_4 up to 200 kilobars, In High pressure research-application to geophysics, edited by M. H. Manghnani and S. Akimoto, pp 255-266, Academic, Orlando, Fla,1977.

Sun, S. S., and R. W. Nesbitt, Petrogenesis of Archean ultrabasic and basic volcanics: evidence from rare earth elements, Contrib. Mineral. Petrol., 65, 301-325,1978.

Takahashi, E., Melting of a dry peridotite KLB-1 up to 14 GPa: Implications on the origin of peridotitic upper mantle, J. Geophys. Res., 91, 9367-9382, 1986.

Takahashi, E., and I. Kushiro, Melting of a dry peridotite at high pressures and basalt magma genesis, Amer. Mineral., 68, 859-879, 1983.

Takahashi, E., and C. M. Scarfe, Melting of peridotite to 14 GPa and genesis of komatiite, Nature, 315, 566-568, 1985.

Takahashi, E., H. Yamada, and E. Ito, An ultrahigh-pressure furnace assembly to 100 kbar and 1500 °C with minimum temperature uncertainty, Geophys. Res. Lett., 9, 805-807, 1982.

Thompson, R. N., Primary basalts and magma genesis, I Skye Northwest Scotland, Contrib. Mineral. Petrol., 45, 317-341, 1974.

Thompson, R. N., and I. Kushiro, The oxygen fugacity within graphite capsules in piston cylinder apparatus at high pressure, Carnegie Inst.Wash. Yearb., 71, 615-616, 1972.

Ulmer, P., The dependence of the Fe^{2+}-Mg cation-partitioning between olivine and basaltic liquid on pressure, temperature and composition: An experimental study to 30 kbars, Contrib. Mineral. Petrol.,101, 261-273, 1989.

Viljoen M. J., and R. P. Viljoen, Evidence for the existence of mobile extrusive peridotitic magma from the Komati Formation of the Onverwacht group, Geol. Soc. S. Afr. Spec. Publ., 2, 87-112, 1969a.

Viljoen, M. J., and R. P. Viljoen, The geology and geochemistry of lower ultramafic unit of the Onverwacht group and a proposed new class of igneous rocks, Geol. Soc. S. Afr. Spec. Publ., 2, 55-86, 1969b.

Viljoen, R. P., and M. J. Viljoen, The effects of metamorphism and serpentinization on the volcanic and associated rocks of Barberton region, Geol. Soc. S. Afr. Spec. Publ., 2, 29-54, 1969c.

Viljoen, M. T., R. P. Viljoen and T. N. Pearton, The nature and distribution of Archean komatiite volcanic in South Africa, in komatiites, edited by N. T. Arndt and E. G. Nisbet, pp 53-79, George Allen and Unwin, London, 1982.

Visser, W., and A. F. Koster Van Groos, Phase relations in the system K_2O-FeO-Al_2O_3-SiO_2 at 1 atmosphere with special emphasis on low temperature liquid immiscibility, Amer. J. Sci., 279, 70-91, 1979.

Walker, D., S. Jurewicz, and E. B. Watson, Adcumulus dunite growth in a laboratory thermal gradient, Contrib. Minral. Petrol., 99, 306-319, 1988.

Williams, D. A. C., Archaean ultramafic, mafic and associated rocks, Mt. Monger, Western Australia, J. Geol. Soc. Aust., 19, 163-188, 1972.

Williams, D. A. C., and R. G. Furnell, Reassessment of part of the Barberton type area, South Africa, Precambrian Res., 9, 325-347, 1979.

Wyllie, P. J., Constraints imposed by experimental petrology on possible and impossible magma sources and products, Phil. Trans. R. Soc. London, A-310, 439-456, 1984.

Wyllie, P. J., C. H. Donaldso, A. J. Irving, S. E. Kesson, R. B. Merrill, D. C. Presnall, E. M. Stolper, T. M. Usselman, and D. Walker, Experimental petrology of basalts and their source rocks, Chapter 3 (pp 493-630), in Basaltic Volcanisim on the Terrestrial Planets, Pergamon, New York, 1981.

Yagi, T., M. Akaogi, M. Arashi, T. Okai, K. Kawamura, K. Shino, M. Shimomura, T. Suzuki, K. Tabata, and S. Akimoto, Precise determination of olivine-spinel phase transformation in Fe_2SiO_4, J. Geophys. Res., 92, 6207-6213, 1987.

Yamada, H., and E. Takahashi, Subsolids phase relations between ccexisting garnet and two pyroxene at 50 to 100 kbar in the system CaO-MgO-Al_2O_3-SiO_2, in Kimberlites II, edited by Koroprobst: The mantle and crust-mantle relationships, pp 247-255, 1984.

Zindler, A., Nd and Sr isotopic studies of komatiites and related rocks, in Komatiites, edited by N. T. Arndt and E. G. Nisbet, pp 399-421, George Allen and Unwin, London, 1982.